ISSN 1674-1056
http://cpb.iphy.ac.cn
http://iopscience.iop.org/cpb
中国物理 B
Chinese Physics
中国物理 Chinese Physics B

A passive source ranging method based on the frequency warping transform of the vertical intensity flux in shallow water

Yu-Bo Qi(戚聿波), Shi-Hong Zhou(周士弘), Meng-Xiao Yu(于梦枭), Shu-Yuan Du(杜淑媛), Mei Sun(孙梅), Ren-He Zhang(张仁和)

Citation: Chin. Phys. B . 2019, 28(5): 054302. **doi:** 10.1088/1674-1056/28/5/054302
Journal homepage: http://cpb.iphy.ac.cn; http://iopscience.iop.org/cpb

What follows is a list of articles you may be interested in

Spatial correlation of the high intensity zone in deep-water acoustic field

Jun Li(李鋆), Zheng-Lin Li(李整林), Yun Ren(任云)
Chin. Phys. B . 2016, 25(12): 124310. **doi:** 10.1088/1674-1056/25/12/124310

A three-dimensional coupled-mode model for the acoustic field in a two-dimensional waveguide with perfectly reflecting boundaries

Wen-Yu Luo(骆文于), Xiao-Lin Yu(于晓林), Xue-Feng Yang(杨雪峰), Ze-Zhong Zhang(张泽众), Ren-He Zhang(张仁和)
Chin. Phys. B . 2016, 25(12): 124309. **doi:** 10.1088/1674-1056/25/12/124309

Analytical solution based on the wavenumber integration method for the acoustic field in a Pekeris waveguide

Wen-Yu Luo(骆文于), Xiao-Lin Yu(于晓林), Xue-Feng Yang(杨雪峰), Ren-He Zhang(张仁和)
Chin. Phys. B . 2016, 25(4): 044302. **doi:** 10.1088/1674-1056/25/4/044302

Investigation of long-range sound propagation in surface ducts

Duan Rui, Yang Kun-De, Ma Yuan-Liang
Chin. Phys. B . 2013, 22(12): 124301. **doi:** 10.1088/1674-1056/22/12/124301

Benchmark solutions for sound propagation in an ideal wedge

Luo Wen-Yu, Yang Chun-Mei, Qin Ji-Xing, Zhang Ren-He
Chin. Phys. B . 2013, 22(5): 054301. **doi:** 10.1088/1674-1056/22/5/054301

A passive source ranging method based on the frequency warping transform of the vertical intensity flux in shallow water*

Yu-Bo Qi(戚聿波)[1,†], Shi-Hong Zhou(周士弘)[1], Meng-Xiao Yu(于梦枭)[1], Shu-Yuan Du(杜淑媛)[1], Mei Sun(孙梅)[2], and Ren-He Zhang(张仁和)[1]

[1] State Key Laboratory of Acoustics, Institute of Acoustics, Chinese Academy of Sciences, Beijing 100190, China
[2] School of Physics and Electronic Engineering, Taishan University, Taian 271000, China

(Received 23 November 2018; revised manuscript received 25 February 2019; published online 20 March 2019)

The phase of cross-correlation function of two different normal modes contains source range information, which can be extracted by warping transform due to the dispersive characteristics of the shallow water waveguide. The autocorrelation function of the received pressure or particle velocity contains both modal autocorrelation component (MAC) and modal cross-correlation component (MCC), with the former part usually treated as interference for source ranging. Because the real part of the vertical intensity flux (RPVIF) only contains MCC, a passive impulsive source ranging method based on the frequency warping transform of RPVIF with a single vector receiver in shallow water is presented. Using a waveguide-invariant-based frequency warping operator, the cross-correlation components of two different modes in the vertical intensity flux are warped into separable impulsive sequences, the time delays of which are subsequently used for source ranging. The advantages of source ranging based on warping the vertical intensity flux compared with warping the pressure autocorrelation function are pointed out, and the experiment results are also presented.

Keywords: passive source ranging, vertical intensity flux, frequency warping transform, normal mode

PACS: 43.30.Wi, 43.30.Bp, 43.60.Jn **DOI:** 10.1088/1674-1056/28/5/054302

1. Introduction

In a low-frequency shallow water waveguide, the acoustic field is always dominated by a set of normal modes that propagate dispersively, with each frequency component traveling with different group speed.[1] Thus, at a sufficiently large distance away from the source, each mode can be separated in the time–frequency domain of the received signal. The information carried by each mode can then be used for source localization and geoacoustic inversion. However, due to the limit of time frequency resolution, simple time–frequency analysis is unsuitable for modal filtering at relatively close ranges. It has been recently demonstrated that normal mode filtering can be successfully achieved by combining traditional time–frequency analysis and warping transform.[2]

Warping transform is a unitary transform, and was first introduced to signal analysis by Baraniuk.[3] If an expression for every mode in time/frequency is obtained, then the original signal can be transformed into monotones with different frequency or impulsive sequences with different time delays using a corresponding time/frequency warping operator through time/frequency nonlinear resampling. Based on the expression for the mode's instantaneous phase in time domain of an ideal waveguide model, the warping operator $h(t)=\sqrt{t^2+t_{\rm r}^2}$ is proposed to filter normal modes from the signal received by a single hydrophone, where $t_{\rm r}$ is the arrival time of a signal.[2] This time warping operator has been used for numerous applications, including geoacoustic inversion,[2,4–7] marine mammals or impulsive source localization,[8–11] even in a range-dependent shallow-water waveguide.[12] It should be noted that all the above analyses are confined to impulsive sources if the signal to be warped is the raw received signal. It is necessary to deconvolute the influence of the source characteristic for non-impulsive sources. To properly apply frequency warping transform, the time coordinate at the receiver must be aligned with the source time coordinate, and it is unpractical for passive receiving system without a couple of arrival time attempts as the receiver continuously records without any knowledge of when, or even if, the non-cooperative source transmits.

One should note that the traditional warping operator $h(t)=\sqrt{t^2+t_{\rm r}^2}$ is only suitable for the shallow water waveguide with reflecting-dominated modes. In other words, it is valid for the shallow water waveguides with waveguide invariant approximately equal to 1. In the waveguide with a strong thermocline or a surface channel, the waveguide invariant varies over a range of values, thus the effect of warping operator $h(t)=\sqrt{t^2+t_{\rm r}^2}$ will significantly decline. So the waveguide-invariant-based warping operators suitable for reflecting-dominated or refracted-dominated modes are proposed.[13–15]

Warping the autocorrelation function of the pressure/particle velocity or the cross-correlation function of the pressure and particle velocity eliminates the source phase's

*Project supported by the Frontier Science Research Project of Chinese Academy of Sciences (Grant No. QYZDY-SSW-SLH005).
†Corresponding author. E-mail: qyb@mail.ioa.ac.cn
© 2019 Chinese Physical Society and IOP Publishing Ltd

effect and the uncertainty of signal arrival time, thus it avoids the confine of impulsive sources and alignment of the receiver–source time coordinate.[15] Besides, the modal cross-correlation component (MCC) in the signal autocorrelation function has similar dispersive characteristics compared to the mode itself.[8,9] In most cases, the mode's autocorrelation component (MAC) is concentrated near the time of zero compared with the MCC, and zeroing this part of the signal autocorrelation can delete it to a large extent.[13] However, for the signal received at very close ranges, this method cannot delete it ideally because the MCC and MAC overlap in time. Thus, good modal cross-correlation component filtering and source ranging results are difficult to achieve.

The warping transform of the vector field is firstly analyzed in Ref. [16], but the joint warping of the pressure and particle velocity is not concerned. As the real part of the vertical intensity flux only contains modal cross-correlation component,[17] the frequency warping transform and its use for passive source ranging are presented.

The rest of this paper is organized as follows. Section 2 presents theoretical analyses including the expression of the vertical intensity flux described by the waveguide invariant, the corresponding frequency warping transform, and the passive source ranging method. In Section 3, the frequency warping transform and source ranging method are applied on real data. Finally, the conclusion is provided in Section 4.

2. Theoretical analyses

According to the normal mode theory, the received pressure and particle vertical velocity at depth z after propagation over a range r in a range-independent shallow water waveguide can be expressed as[1]

$$P(r,z,f)=\sum_{m=1}^{M}P_m(r,z,f)\mathrm{e}^{\mathrm{j}k_{rm}(f)r}, \tag{1}$$

$$V_z(r,z,f)=\sum_{m=1}^{M}V_{zm}(r,z,f)\mathrm{e}^{\mathrm{j}k_{rm}(f)r}, \tag{2}$$

where $k_{rm}(f)$ represents the modal horizontal wavenumber at frequency f, M denotes the number of propagating modes, $P_m(r,z,f)$ and $V_{zm}(r,z,f)$ are the amplitudes of mode m in pressure and vertical velocity,

$$P_m(r,z,f)=\frac{S(f)\mathrm{j}\mathrm{e}^{-\mathrm{j}\pi/4}}{\rho(z_\mathrm{s})\sqrt{8\pi r k_{rm}(f)}}\psi_m(z_\mathrm{s})\psi_m(z), \tag{3}$$

$$V_{zm}(r,z,f)=\frac{S(f)\mathrm{e}^{-\mathrm{j}\pi/4}}{\rho(z)\rho(z_\mathrm{s})2\pi f\sqrt{8\pi r k_{rm}(f)}}\psi_m(z_\mathrm{s})\psi'_m(z). \tag{4}$$

Here, $\psi_m(z)$ is the modal depth function of mode m, $S(f)$ is the source spectrum, $\rho(z)$ represents the water density at depth z, and $\psi'_m(z)$ is the derivative with respect to z. Due to the difference of $\psi'_m(z)$ and $\psi_m(z)$, the energy ratio of each mode in vertical velocity is different from that of the pressure. According to Eqs. (1) and (2), the autocorrelation functions of the pressure and the vertical velocity can be expressed as

$$\begin{aligned}I_{PP}(r,z,f)&=P(r,z,f)P^*(r,z,f)\\&=\sum_{m=1}^{M}|P_m|^2+\sum_{m=1}^{M}\sum_{n\neq m}^{M}P_mP_n^*\mathrm{e}^{\mathrm{j}\Delta k_{nn}r},\end{aligned} \tag{5}$$

$$\begin{aligned}I_{V_zV_z}(r,z,f)&=V_z(r,z,f)V_z^*(r,z,f)\\&=\sum_{m=1}^{M}|V_{zm}|^2+\sum_{m=1}^{M}\sum_{n\neq m}^{M}V_{zm}V_{zn}^*\mathrm{e}^{\mathrm{j}\Delta k_{mn}r},\end{aligned} \tag{6}$$

where $\Delta k_{mn}=k_{rm}(f)-k_{rn}(f)$, and the superscript asterisk denotes the complex conjugation operator. The first part is the sum of all modes' autocorrelation component, while the second part represents the cross-correlation component of different modes.

According to Eqs. (1)–(4), the vertical intensity flux can be written as

$$\begin{aligned}I_{PV_z}(r,z,f)&=P(r,z,f)V_z^*(r,z,f)\\&=\frac{\mathrm{j}}{2\pi f\rho(z)}\left(\sum_{m=1}^{M}\frac{\psi'_m(z)}{\psi_m(z)}|P_m|^2\right.\\&\quad\left.+\sum_{m=1}^{M}\sum_{n\neq m}^{M}\frac{\psi'_n(z)}{\psi_n(z)}P_mP_n^*\mathrm{e}^{\mathrm{j}\Delta k_{mn}r}\right).\end{aligned} \tag{7}$$

The first imaginary part is the sum of all modes' autocorrelation function, while the second complex part represents the cross-correlation function of different modes. Thus, the real part of the vertical intensity flux is

$$I_{PV_z}^{\mathrm{real}}(r,z,f)=\frac{-1}{\rho(z)2\pi f}\sum_{m=1}^{M}\sum_{n\neq m}^{M}\frac{\psi'_n(z)}{\psi_n(z)}P_mP_n^*\sin\Delta k_{mn}r, \tag{8}$$

and the imaginary part is

$$\begin{aligned}I_{PV_z}^{\mathrm{imag}}(r,z,f)&=\frac{1}{\rho(z)2\pi f}\left(\sum_{m=1}^{M}\frac{\psi'_m(z)}{\psi_m(z)}|P_m|^2\right.\\&\quad\left.+\sum_{m=1}^{M}\sum_{n\neq m}^{M}\frac{\psi'_n(z)}{\psi_n(z)}P_mP_n^*\cos\Delta k_{mn}r\right).\end{aligned} \tag{9}$$

One can note that $I_{PV_z}^{\mathrm{real}}(r,z,f)$ only contains MCC while $I_{PV_z}^{\mathrm{imag}}(r,z,f)$ contains both MAC and MCC.

The mode wavenumber difference and the frequency satisfy the following power law relationship:[18]

$$\Delta k_{mn}(f)=\gamma_{mn}f^{-1/\beta}, \tag{10}$$

where β is the waveguide invariant and γ_{mn} represents a mode dependent constant. Inserting Eq. (10) into Eq. (8) and simplifying the equation, we have

$$I_{PV_z}^{\mathrm{real}}(r,z,f)=\sum_{m=1}^{M}\sum_{n\neq m}^{M}A_{mn}(f)\left(\mathrm{e}^{\mathrm{j}r\gamma_{mn}f^{-1/\beta}}-\mathrm{e}^{-\mathrm{j}r\gamma_{mn}f^{-1/\beta}}\right), \tag{11}$$

where

$$A_{mn}(f)=\frac{\mathrm{j}}{\rho(z)4\pi f}\frac{\psi'_n(z)}{\psi_n(z)}P_mP_n^*.$$

According to Eq. (11), using the waveguide-invariant-based frequency warping operator $w(f) = Cf^{-\beta}$,[15] $I^{\text{real}}_{PV_z}(r,z,f)$ can be warped into

$$\text{FW}\left[I^{\text{real}}_{PV_z}(r,z,f)\right] = \sqrt{\left|\frac{\mathrm{d}w(f)}{\mathrm{d}f}\right|}\sum_{m=1}^{M}\sum_{n\neq m}^{M} A_{mn}(Cf^{-\beta}) \times (\mathrm{e}^{\mathrm{j}r\gamma_{mn}C^{-1/\beta}f} - \mathrm{e}^{-\mathrm{j}r\gamma_{mn}C^{-1/\beta}f}), \quad (12)$$

where C is a constant to ensure that the warped frequency band has the biggest overlapping part with the original signal frequency band from f_1 to f_2.[15] As shown in Eq. (12), only after one time transformation, all modal cross-correlation components in $I^{\text{real}}_{PV_z}(r,z,f)$ are warped into separable impulsive sequences with time delay which equals

$$t_{mn} = \pm r\gamma_{mn}C^{-1/\beta}/2\pi, \quad (13)$$

when the source spectrum amplitude $|S(f)|$ is flat and the amplitude of $A_{mn}(Cf^{-\beta})$ is considered to be a slowly varying function of frequency compared to the phase dependence. It should be noted that the waveguide-invariant-based warping operator is suitable for reflecting-dominated or refracted-dominated modes when the waveguide invariant can be treated as a single value. For the waveguide with both reflecting and refracted modes, pre-processing to filter these two types of modes is needed. Otherwise, the refracted modes are interference for warping the reflecting modes and vice versa.

According to Eq. (13), the target source range can be estimated by

$$r = \pm 2\pi t_{mn}/\gamma_{mn}C^{-1/\beta}. \quad (14)$$

The mode dependent constant γ_{mn} in Eq. (14) can be obtained by curve fitting according to Eq. (10) when the waveguide environmental parameters are known to calculate $\Delta k_{mn}(f)$, or obtained from a guide source with known range r_{g} and the corresponding time delay t_{gmn} of the warped $I^{\text{real}}_{PV_z}(r_{\text{g}},z,f)$. More briefly, because the time delay t_{mn} increases linearly with range r, the target source range can be estimated by

$$r = \frac{t_{mn}}{t_{gmn}} r_{\text{g}}, \quad (15)$$

when a guide source is available. Equation (15) gives the source ranging result of one modal cross-correlation component; if there are multiple modal cross-correlation components in the vertical intensity flux, the estimated source range can be chosen as their mean value. Thus, target source range can be achieved by following the steps below.

(i) Obtain the pressure $P(r,z,f)$ and particle vertical velocity $V_z(r,z,f)$ through Fourier transform of the received signal in time domain.

(ii) Obtain the real part of the vertical intensity flux $I^{\text{real}}_{PV_z}(r,z,f)$ according to Eq. (7).

(iii) Warp $I^{\text{real}}_{PV_z}(r,z,f)$ using the waveguide-invariant-based frequency warping operator $w(f) = Cf^{-\beta}$, i.e., get $\text{FW}\left[I^{\text{real}}_{PV_z}(r,z,f)\right]$ through no-linear resampling $I^{\text{real}}_{PV_z}(r,z,f)$ in frequency domain.

(iv) Obtain the waveform of the warped real part of the vertical intensity flux, i.e., $\text{IFFT}\left\{\text{FW}\left[I^{\text{real}}_{PV_z}(r,z,f)\right]\right\}$, through inverse Fourier transform of $\text{FW}\left[I^{\text{real}}_{PV_z}(r,z,f)\right]$.

(v) Get the time delay t_{mn} of the peaks in $\text{IFFT}\left\{\text{FW}\left[I^{\text{real}}_{PV_z}(r,z,f)\right]\right\}$ and estimate the source range according to Eq. (15). If multiple modal cross-correlation components are available, use their average value as the final estimated result.

3. Experimental results

To testify the validity of this analysis, the experimental data recorded in the North Yellow Sea in the winter of 2008 is processed. As shown in Fig. 1, the airgun source is towed at 10.5 m and the water depth is 32.5 m. The sound speed profile is iso-speed of 1521 m/s. The received signals are recorded by a vector sensor deployed at a depth of 18.1 m.

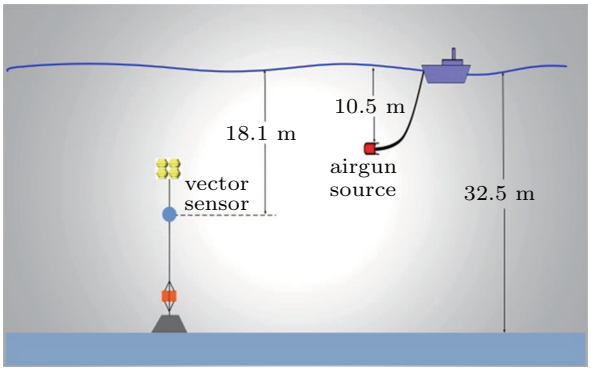


Fig. 1. Configuration of the experiment.

The adaptive optimal kernel time–frequency representations of an impulsive signal (as shown in Figs. 2(a) and 2(b)) recorded by the pressure and vertical velocity channel with the source-receiver range equal to 5 km are shown in Figs. 2(c) and 2(d). On each subfigure, the modes are labeled to ease the reading. As shown in Figs. 2(c) and 2(d), the pressure and vertical velocity contain different modes. The pressure field contains modes 1, 2, 3, and 5 with mode 1 having the greatest contribution, while the vertical velocity contains modes 2 and 4 with mode 2 dominating the field.

Due to the dispersive characteristics of the normal mode as shown in Fig. 2, both the time spread lengths of MAC and MCC are related to the source frequency, source range, and mode number. Comparing with the cross-correlation component, most energy of the modal autocorrelation component is concentrated closer to the time zero with a smaller time spread length, so zeroing the signal autocorrelation near the peak (i.e.,

near the time zero) can delete it to a large extent when the source is relatively far away. However, with the increase of frequency band and mode number, as well as the decrease of source range, the energy of MAC and MCC overlapping in time domain increases, so zeroing the signal autocorrelation near the peak is not an ideal way to delete the interference component (i.e., the modal autocorrelation component) for warping.

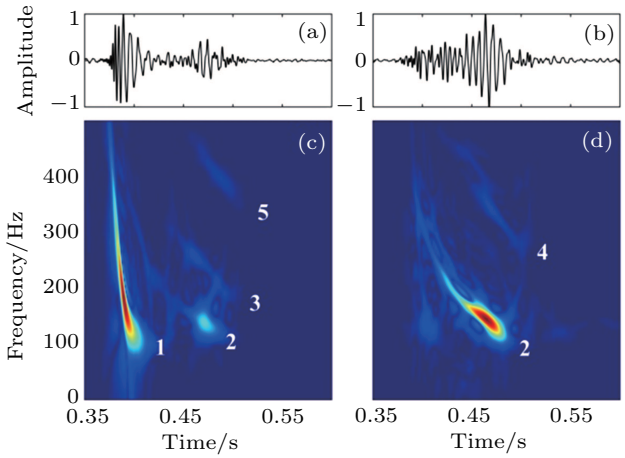


Fig. 2. The received signals and their time–frequency representations. (a) Normalized waveform of the received pressure, (b) normalized waveform of the received vertical velocity, (c) spectrogram of the received pressure, and (d) spectrogram of the received vertical velocity. In every subfigure, the mode numbers are labeled in white. The spectrogram color scale is linear and arbitrary.

The unwarped and warped I_{PP} received at different ranges are presented in Fig. 3 under two conditions, 0 s zeroing length and 0.01 s zeroing length. Because the water sound speed is iso-speed, the waveguide invariant equal to 1 is used in the frequency warping operator. As shown in Fig. 3(b), the warped MCC is not apparent due to the existence of a much brighter vertical line corresponding to the MAC, implying that the energy of MAC is much bigger than that of MCC. After setting the signal autocorrelation before 0.01 s to zero to delete the MAC, there is a bright oblique line in Fig. 3(d) corresponding to the cross-correlation of modes 1 and 2. Compared with the long time spread in Fig. 3(c), MCC is almost warped into impulsive sequence in Fig. 3(d). But for the ranges within 2.5 km, this line is intermittent due to the unsatisfactory result of zeroing.

For comparison, figure 4 presents the waterfall plot of unwarped and warped vertical intensity flux at different ranges with 0 s zeroing length. The first row is the real part while the second row is the imaginary part. From Figs. 4(b) and 4(d), we can conclude that both the real and imaginary parts of I_{PV_Z} are transformed into impulsive sequences with the time delay increasing linearly with the source range. Comparing with warped I_{PP} in Fig. 3(d), warped I_{PV_Z} presents a straighter and cleaner line corresponding to the cross-correlation of modes 1 and 2. For the ranges smaller than 2.5 km, this line is still straight. Because the pressure and vertical velocity contains different modes, even for the imaginary part of vertical energy flux, the energy of MCC is much bigger than MAC; thus, figure 4(d) presents a same oblique bright line as Fig. 4(b).

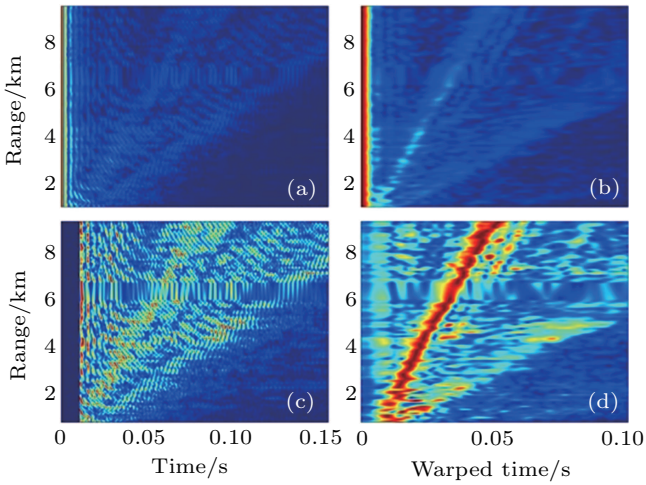


Fig. 3. Waterfall plot of the unwarped and warped pressure autocorrelation function at different ranges. (a) Unwarped pressure autocorrelation function with 0 s zeroing length, (b) warped pressure autocorrelation function with 0 s zeroing length, (c) unwarped pressure autocorrelation function with 0.01 s zeroing length, and (d) warped pressure autocorrelation function with 0.01 s zeroing length.

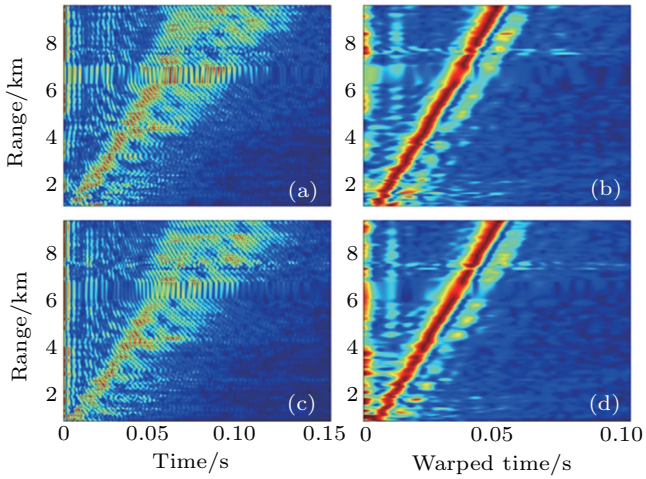


Fig. 4. Waterfall plot of the unwarped and warped vertical intensity flux at different ranges with 0 s zeroing length. (a) Unwarped real part of the vertical intensity flux, (b) warped real part of the vertical intensity flux, (c) unwarped imaginary part of the vertical intensity flux, and (d) warped imaginary part of the vertical intensity flux.

The estimated source ranges based on the time delay of the impulsive sequences are given in Fig. 5, where the blue circled line is the result of warped $I^{\text{real}}_{PV_z}(r,z,f)$ and the black asterisk line is the result of warped I_{PP}. Here, the source emitted at 5 km is chosen as the guide source, the time delay of which is 0.0267 s. As the energy ratio of each mode in the signal excited by the guide source and that of the target source is the same, the target source range can be estimated directly according to Eq. (15) without mode number identification. As shown in Fig. 5, the blue circled result is much better than the

black asterisk result, especially for the ranges within 2.5 km, resulting from the fact that the warped I_{PV_Z} gives a straighter and cleaner line.

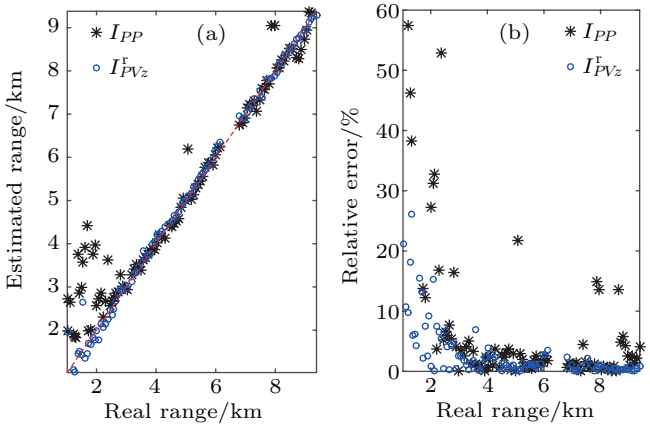


Fig. 5. Source ranging results. (a) Estimated range vs. real range. (b) Relative error.

4. Summary

A passive source ranging method using the time delays of the peaks in the frequency warped vertical intensity flux is presented. Compared with warping the pressure autocorrelation function, there is no need to delete the modal autocorrelation component for warping the vertical intensity flux, especially for its real part. In addition, the source ranging result based on the time delay of the warped vertical intensity flux is much better for closer ranges.

One should note that the mode number identification is usually needed before source ranging, to make sure that the same combination of two modes is used for the guide source and the target source. Otherwise, the estimated source range is a wrong value, which is similar to the estimated result of the matched field processing sometimes positioned at the false peak of the cost function due to the similarity of the acoustic field. In more practical application scenarios, because the mode amplitude is directly related to the source depth and their difference is small for similar tonnage ships, the dominated modes excited by two ships with similar tonnage are same at the same frequency band. Thus, one can use a cooperative surface ship as the guide source to estimate the ranges of other non-cooperative surface ships. Another point that should be noted is the amplitude of the ship radiated noise spectrum because its considerable fluctuation will have a devastating effect on warping transform. For the engineering application of the source ranging method proposed in this paper, further research and more endeavors are needed to get stable, usable, and identifiable modal cross-correlation components.

References

[1] Jensen F B, Kuperman W A, Porter M B and Schmidt H 1994 *Computational Ocean Acoustics* (New York: AIP publishing)
[2] Bonnel J, Nicolas B, Mars J I and Walker S C 2010 *J. Acoust. Soc. Am.* **128** 719
[3] Baraniuk R and Jones D 1995 *IEEE Trans. Signal Process.* **43** 2269
[4] Bonnel J and Chapman N R 2011 *J. Acoust. Soc. Am.* **130** EL101
[5] Bonnel J, Dosso S E and Ross Chapman N 2013 *J. Acoust. Soc. Am.* **134** 120
[6] Zeng J, Chapman N R and Bonnel J 2013 *J. Acoust. Soc. Am.* **134** EL394
[7] Bonnel J, Lin Y T, Eleftherakis D, Goff J A, Dosso S, Chapman R, Miller J H and Potty G R 2018 *J. Acoust. Soc. Am.* **143** EL405
[8] Zhou S H, Qi Y B and Ren Y 2014 *Sci. Chin.: Ser. G* **57** 225
[9] Qi Y B, Zhou S H, Ren Y, Liu J J, Wang D J and Feng X Q 2015 *Acta Acustica* **40** 144 (in Chinese)
[10] Bonnel J, Thode A, Blackwell S, Kim K and Macrander A 2014 *J. Acoust. Soc. Am.* **136** 145
[11] Thode A, Bonnel J, Thieury M, Fagan A, Verlinden C, Wright D, Berchok C and Crance J 2017 *J. Acoust. Soc. Am.* **141** 3059
[12] Qi Y B, Zhou S H, Zhang R H, Zhang B and Ren Y 2014 *Acta Phys. Sin.* **63** 044303 (in Chinese)
[13] Qi Y B, Zhou S H, Zhang R H and Ren Y 2015 *J. Comput. Acoust.* **23** 1550003
[14] Qi Y B, Zhou S H and Zhang R H 2016 *Acta Phys. Sin.* **65** 134301 (in Chinese)
[15] Qi Y B, Zhou S H, Zhang R H and Ren Y 2015 *Acta Phys. Sin.* **64** 074301 (in Chinese)
[16] Zhu L M, Li F H, Sun M and Chen D S 2015 *Acta Phys. Sin.* **64** 154303 (in Chinese)
[17] Ren Q Y, Hermand J P and Piao S C 2010 *Oceans* 2010 *MTS/IEEE Seattle*, September 20–23, 2010 Seattle, USA
[18] Grachev G A 1993 *Acoust. Phys.* **39** 33